HHS Public Access

Author manuscript

Int J Radiat Oncol Biol Phys. Author manuscript; available in PMC 2022 April 01.

Published in final edited form as:

Int J Radiat Oncol Biol Phys. 2021 April 01; 109(5): 1647–1656. doi:10.1016/j.ijrobp.2020.12.014.

Integration of risk survival measures estimated from pre- and post-treatment CT scans improves stratification of early stage non-small cell lung cancer patients treated with stereotactic body radiation therapy

Zhicheng Jiao[*], **Hongming Li**[*], **Ying Xiao**[♫], **Charu Aggarwal**[§], **Maya Galperin-Aizenberg**[*], **Daniel Pryma**[*], **Charles B. Simone II**[♪,#], **Steven J. Feigenberg**[♫], **Gary D. Kao**[♫], **Yong Fan**[*]

[*]Department of Radiology, Perelman School of Medicine, University of Pennsylvania, Philadelphia, PA 19104, United States

[♫]Department of Radiation Oncology, Perelman School of Medicine, University of Pennsylvania, Philadelphia, PA 19104, United States

[§]Division of Hematology and Oncology, Department of Medicine, University of Pennsylvania, Philadelphia, PA 19104, United States

[♪]New York Proton Center, New York, NY 10035, United States

[#]Memorial Sloan Kettering Cancer Center, New York, NY 10035, United States

Abstract

Purpose: To predict overall survival of patients receiving stereotactic body radiation therapy (SBRT) for early-stage non-small cell lung cancer (ES-NSCLC), we developed a radiomic model that integrates risk of death estimates and changes based on pre- and post-treatment CT scans. We hypothesize this innovation will improve our ability to stratify patients into various oncologic outcomes with greater accuracy.

Experimental design: Two cohorts of ES-NSCLC patients uniformly treated with SBRT (a median dose of 50Gy in 4–5 fractions) were studied. Prediction models were built on a discovery cohort of 100 patients with treatment planning CT scans, and then were applied to a separate validation cohort of 60 patients with pre- and posttreatment CT scans for evaluating their performance.

Results: Prediction models achieved a c-index up to 0.734 in predicting survival outcomes of the validation cohort. The integration of the pre-treatment risk of survival measures (Risk-High vs.

Corresponding author: Yong Fan, PhD, Associate Professor, Center for Biomedical Image Computing and Analytics (CBICA), Department of Radiology, University of Pennsylvania, Richards Building, 7th Floor, 3700 Hamilton Walk, Philadelphia, PA 19104, Tel: 215-746-4065, yong.fan@pennmedicine.upenn.edu, yong.fan@ieee.org. **Authors responsible for statistical analysis:** Zhicheng Jiao, Zhicheng.jiao@pennmedicine.upenn.edu.

Data sharing

Research data are not available at this time.

Risk-Low) and changes (Risk-Increase vs. Risk-Decrease) in risk of survival measures between the pre-treatment and post-treatment scans further stratified the patients into 4 subgroups (Risk: high, increase; Risk: high, decrease; Risk: low, increase; Risk: low, decrease) with significant difference (χ^2 = 18.549, p=3.4e-04, log-rank test). There was also significant difference between risk increase and risk decrease group (χ^2= 6.80, p=0.0091, log-rank test). In addition, significant difference (χ^2= 7.493, p=0.0062, log-rank test) was observed between the high-risk and low-risk groups obtained based on the pre-treatment risk of survival measures.

Conclusion: The integration of risk of survival measures estimated from pre- and post-treatment CT scans can help differentiate patients with good expected survival from those who will do more poorly following SBRT. The analysis of these radiomics-based longitudinal risk measures may help identify early stage NSCLC patients who will benefit from adjuvant treatment after lung SBRT, such as immunotherapy.

Introduction

Lung cancer causes the greatest number of cancer-related deaths in the United States, and non-small cell lung cancer (NSCLC) accounts for the overall majority (approximately 87 percent), with poor treatment outcomes and a low 5-year survival rate (1–3).The advance in lung cancer screening technologies has facilitated detection of more tumors in early cancer stage (4,5). Those diagnosed with early stage (ES)-NSCLC are now more likely to receive definitive treatment with the increased utilization of convenient and effective hypofractionated radiotherapy such as stereotactic body radiation therapy (SBRT) that is also referred to as stereotactic ablative radiotherapy (6–8). Consistently encouraging outcomes with SBRT have led to several large-scale efforts to compare SBRT with surgery, the latter considered the existing standard of care (9,10). Several recent reports have not only indicated that oncologic outcomes between SBRT and surgery are similar, but also that SBRT may be safer for at least some patients (11).

However, despite excellent initial local control, up to half of patients with ES-NSCLC will fail regionally and/or distantly within five years after SBRT (8,12,13). In order to improve the outcome of patients with ES-NSCLC, there is an opportunity to add treatment after SBRT. Consequently, optimized methods to guide subsequent treatment throughout each patient’s clinical course is critically needed (14–16).

Radiomics provides promising novel biomarkers towards predicting clinical outcomes (17–21). There has been phenomenal growth of published radiomic studies of lung cancer for the prediction of treatment responses, patient stratification, and prognosis based on radiological imaging data (22–30). Particularly, radiomic features extracted from CT images have demonstrated promising performance for the prediction of overall survival and disease-free survival in patients with NSCLC (31–35). Moreover, changes in radiomic features, often referred to as delta-radiomics features, computed from images during therapy are stable (36) and have also demonstrated prognostic potential specifically in lung cancer (37–39). However, most studies to date have only assessed imaging scans at baseline or from radiation treatment planning before or during therapy, hampering the applicability of delta-radiomics.

In order to evaluate whether integration of standard radiomics and delta-radiomics help predict overall survival of ES-NSCLC patients treated with SBRT, we developed a radiomic model to integrate risk of death estimates based on pre- and post-treatment CT scans in patients receiving stereotactic body radiation therapy (SBRT). We hypothesize that our radiomic-based longitudinal risk analysis will allow us to stratify patients with various overall survival outcomes with greater accuracy.

Materials and methods:

1. Patients and clinical characteristics

This study was carried out with the approval of our institutional review board. Two cohorts of ES-NSCLC patients treated with SBRT were included in this study. The first cohort contained 100 patients who were treated from July 2009 to June 2013, allowing time for adequate follow-up, and who had pre-treatment CT scans for treatment planning. The second cohort included other 60 patients who were treated from November 2012 to February 2019 and who had both pre-treatment and post-treatment CT scans (Pre-treatment period: November 2012 to March 2017; Post-treatment period: April 2013 to February 2019). The time interval between SBRT and post-treatment CT was 6.2 ± 4.8 months (mean ± standard deviation). These patients were examined on CT scanners of Phillips Gemini TF TOF 16 (Phillips Medical Systems, Amsterdam, Netherlands) at our institute. All patients underwent a free breathing scan and 4D scan using an 8-bin approach, no motion mitigation was performed during the time frame of patients treated on this study. Axial images were obtained using a 3 mm slice thickness encompassing the entire thorax with matrix size of 512 * 512 with spacing of 1.1719 * 1.1719 mm^2. Both the pre- and post-treatment CT scans were collected using the same imaging protocol.

Each patient has a predominant solid component of their NSCLC that was delineated as gross tumor target volume (GTV) in CT scans (pre-treatment CT for cohort 1, pre- and post-treatment CT for cohort 2) by board certified thoracic radiation oncologists. Following existing studies (30,40–42), we used GTV as a region of interest to compute radiomic features in our study.

Although all patients in the involved cohorts were treated uniformly with SBRT, they had different primary tumor appearances and treatment outcomes. Particularly, the median of prescription dose was 50 Gy with a range of 50–60 Gy), and the median range of fractions was 4 or 5 fractions with a range of 4–20 fractions. Prescription isodose line was 80–100% as a range with 85–90% median. BED10 was 100 Gy if 5 fractions and 112.5 Gy if 4 fractions, and the range was 78–112.5 Gy. The vast majority of patents received 4 or 5 fraction regimens (92%), whereas a handful of additional patients received 8, 15 or 20 fraction regimens, due to the tumors being ultracentrally located and dose constraints with 5 fractions being exceeded. Following treatment, patients were monitored for disease control via computed tomography (CT) or positron emission tomography (PET)/CT imaging every 3 months in accordance with institutional practice. Date of death was determined by death certificates or institutional medical records. The patients had a median follow-up of 2.0 years.

Descriptive statistics were used to evaluate demographic characteristics and disease details. Chi-square for categorical variables, t-test for continuous variables, and log-rank test for time-to-event variables were carried out to examine differences in clinicopathologic details between patients in these two cohorts.

2. Radiomics features and prediction modeling

The construction and application of a radiomic survival prediction model is illustrated in Figure 1. Particularly, we computed 680 radiomics features from the GTV of each CT scan using pyradiomics (43). These quantitative features characterize tumor shape and texture, including (I) first-order tumor image intensity features, (II) shape features of tumor, (III) high-order texture representation, and (IV) multiscale wavelet features. Details of these features are summarized in Supplementary Table 1. The radiomics analysis was carried out following a standard setting (25,44). Specifically, CT images and GTV annotations were resampled to have isotropic voxels of unit dimension (1 mm^3) using linear and nearest neighbor interpolations, respectively; CT image intensities were discretized using equally spaced bins with a bin-width of 25 Hounsfield Units. This discretization step not only reduces image noise, but also normalizes intensities across all patients, allowing for a direct comparison of all calculated textural features between patients. Finally, radiomic features were computed. We did not register the pre- and post-treatment scans since tumors were manually contoured in both the pre- and post-treatment scans.

We built an overall survival prediction model using random survival forest (RSF) model, which is a variation of random forest method capable of modeling right-censored survival/recurrence data (45). As a meta estimator model, RSF can fit a number of survival trees on various sub-samples of a training dataset and uses averaging across all the survival trees to improve the predictive accuracy and to control over-fitting (45). The model was optimized by assigning higher risks to patient with worse survival outcomes according to the input feature vectors. We used the 100-patient cohort with pre-treatment CT scans as our training dataset and optimized parameters of the RSF model using three-fold cross-validation to maximizing survival prediction performance measured with concordance-index (c-index) (46). Particularly, the RSF model has four parameters, including (1) *n_estimators*: number of trees in the forest; (2) *max_depth*: maximum depth of the tree; (3) *min_samples_split*: minimum number of samples required to split an internal node; and (4) *min_samples_leaf*: minimum number of samples required to be at a leaf node. Values of all these parameters were optimized by a three-fold cross-validation procedure of RSF models on the 100-patient cohort. Search ranges of the parameters were: (1) *n_estimators*: [10, 500]; (2) *max_depth*: [1, 5]; (3) *min_samples_split*: [1, 10]; (4) *min_samples_leaf*: [1, 10]. Optimal parameters are presented in Supplementary Table 2. The RSF model was built using scikit-learn (47).

To improve the prediction performance, we adopted four feature selection(ranking) methods (48) to rank the radiomic features based on the training data, including Wilcoxon test based feature selection (WLCX), Mutual information based feature selection (MIFS), Minimum redundancy maximum relevance (MRMR), and T-test score based feature selection (TSCR). Supplementary Figure 2 shows prediction performance of RSF models built upon radiomics

features ranked by these methods. Based on these results, we chose the MRMR method to select top 70% radiomics features and built a RFS model on the training cohort.

We also built overall survival prediction models on: 1) demographic/clinical features, including Age, Sex, Smoker status, and body mass index (BMI); 2) size of tumor; and 3) their combinations, using RSF. The same training procedure as aforementioned was used.

We combined the radiomic prediction model and the prediction model built on demographic/clinical features and tumor size, and then applied the combined model to the 60-patient cohort to estimate risk scores. Particularly, we applied the prediction models to radiomics features extracted from the pre-treatment and the post-treatment CT scans so that each patient had a pre-treatment risk score and a post-treatment risk score. The RSF model prediction performance was evaluated based on the predicted pre-treatment risk scores in terms of c-index.

Finally, we stratified the 60-patient cohort into two groups based on individual patients' pre-treatment risk scores and changes in risk scores before and after the SBRT. Particularly, k-means clustering with two classes was applied to the pre-treatment survival risk scores of the 60 testing patients to discover high-risk and low-risk groups (27 patients were categorized into Risk-High group, while 33 patients were evaluated as Risk-Low ones), and the changes of risk scores (predicted post-treatment risk score minus pre-treatment risk score) was used to obtain the risk change groups (positive values equal to increased risk while negative values stand for decreased risk). According to the prediction results of our RSF model, risks scores of 29 patients increased after receiving the SBRT and the other 31 patients had decreased risk scores.

In order to identify the most important radiomics features for the survival prediction task, we calculated the Breiman-Cutler permutation variable importance (VIMP) (49) as described in (50). The feature importance value of each feature was defined as the mean decrease of c-index resulting from the 100-time random permutation of this feature. A correlation analysis between changes of these features and risk scores of the patients before and after treatment was carried out to investigate how the features change with the predicted risk scores.

Results

Characteristics of the training and testing patient cohorts

Demographic information and clinical characteristics of these two cohorts are summarized in Table 1. No significant differences between the two cohorts were observed in terms of age, sex, smoking history, BMI, tumor size, as well as local, nodal, and distant failure. However, they were different in survival and follow-up length.

Prediction performance

The radiomic model obtained a c-index of 0.691 for predicting overall survival of patients of the validation cohort based on their pre-treatment scans, while the radiomic model obtained a c-index of 0.693 on the training cohort. The prediction models built upon demographic/clinical measures, size of tumor, and their combination obtained c-index values of 0.647,

0.638, and 0.671 respectively on the validation cohort, and c-index values of 0.656, 0.621 and 0.664 respectively on the training cohort. Then, we added the predicted risk scores of the radiomic model and demographic/clinical model to act as a combined prediction model. The combined prediction model obtained the best performance with a c-index of 0.734 on the validation cohort and a c-index of 0.744 on the training cohort.

Patient group and subgroup stratification

The 60-patient cohort was stratified into two groups with significant differences in their overall survival based on pre-treatment risk scores of individual patients estimated by the combined prediction model, as illustrated by the Kaplan-Meier plot in Figure 2(A). A significant difference (χ^2= 7.493, p=0.0062, log-rank test) was observed in overall survival between the high-risk and low-risk groups of patients. Overall survival for patients with risk-increased and risk-decreased risk scores were significantly different (χ^2= 6.80, p=0.0091, log-rank test), as illustrated in Figure 2(B). The integration of the pre-treatment risk (Risk-High vs. Risk-Low) and risk change (Risk-Increase vs. Risk-Decrease) stratified patients into 4 groups (Risk: high, increase; Risk: high, decrease; Risk: low, increase; Risk: low, decrease) with significant difference (χ^2 = 18.549, p=3.4e-04, log-rank test), as illustrated by the Kaplan-Meier plot in Figure 2(C). Pairwise differences of the 4 stratified subgroups are summarized in Table 2.

Important radiomics features for survival prediction

Figure 3 shows the top 10 most important radiomics features and their corresponding importance measures for survival prediction. The most important features for survival prediction included textural features of Inverse Difference Normalized (IDN), Inverse Difference Moment Normalized (IDMN), Informational Measure of Correlation 1 (IMC1), and Zone Percentage (ZP), and shape feature of Maximum 2D Diameter and Minor Axis Length. Most of these features concentrate on describing the region homogeneity and complexity of the textures in tumor areas.

As illustrated in Figure 4 (A), changes of these features were correlated with risk scores before and after treatment. Particularly, 1) the increase of tumor size showed strong correlation (original_shape_Maximum2DDiameterColumn: r = 0.697, p < 0.001; original_shape_MinorAxisLength: r = 0.609, p < 0.001) with the increase of risk scores of patients; 2) the change of Idn and Idmn values were also positively correlated with the increased risks (wavelet-LLH_glcm_Idn: r = 0.709, p < 0.001; original_glcm_Idn: r = 0.689, p < 0.001; wavelet-LLL_glcm_Idn: r = 0.661, p < 0.001; wavelet-LHL_glcm_Idn: r = 0.62, p < 0.001; wavelet-LLH_glcm_Idmn: r = 0.652, p < 0.001; original_glcm_Idmn: r = 0.642, p < 0.001); (3) the change of Imc feature also had positive correlation with the variation of increased risks (wavelet-LLL_glcm_Imc1: r = 0.654, p < 0.001); while change of the original_glszm_ZonePercentage was negatively correlated with the increased risks (r = −0.657, p < 0.001).

Pre- and post-treatment CT scans of representative patients are shown in Figure 4(B). These scans show that patients with increased risk had increased tumor size (original_shape_Maximum2DDiameterColumn, original_shape_MinorAxisLength) and

homogeneity (represented by the Idn and Idmn features), consistent with the quantitative correlation analysis results shown in Figure 4(A).

Discussion

The present study has demonstrated that a prediction model built upon quantitative radiomics features extracted from pre-treatment planning CT scans using random survival forest obtained promising performance for predicting overall survival of ES-NSCLC patients treated by SBRT in an independent evaluation cohort. When combined with demographic/clinical features-based prediction, the survival prediction performance of our model could be further improved. The predicted pre-treatment risk scores clearly stratified the patients into high-risk and low-risk groups with significant difference in their overall survival outcomes. Patients with increased risk scores had significantly worse overall survival than those with decreased risk scores that were estimated based on both pre- and post-treatment CT scans by the prediction model. Moreover, the integration of pre-treatment risk scores and changes in risk scores stratified the patients into 4 subgroups that had significant differences in overall survival, and patients with high pre-treatment risk scores and increased risk scores after the treatment had significantly worse overall survival than those with low pre-treatment risk scores and decreased risk scores after the treatment, indicating that the longitudinal risk analysis helps better predict overall survival.

Different from delta-radiomics prediction models that require to have imaging data at multiple time points for both training and testing datasets, our novel study built a prediction model based on a training dataset with only pre-treatment scans and applied the prediction model to new patients with scans at multiple time points (2 time points in the present study), providing a new means to integrate imaging data collected at multiple time points in radiomics studies. The relatively larger differences in subgroups identified by the integrated pre-treatment risk scores and changes in risk scores compared with differences in subgroups identified by the pre-treatment risk scores or changes in risk scores alone further indicated that the proposed method could improve the prediction of clinical outcomes of ES-NSCLC patients treated by SBRT. This finding was also supported by the fact that some patients with low pre-treatment risk scores may have increased risk scores. For example, 2 patients in the subgroup of Low-increased died with tumor progression at 10 and 15 months, respectively, and 2 patients in the subgroup of High-decreased died of disease both at 13 months.

The feature importance analysis revealed informative radiomic features that contributed more to the prediction modeling, including both shape and texture features. Particularly, the increase of tumor size was scientifically correlated with changes in predicted risk scores. The majority of top ranked informative radiomic features were texture features, such as wavelet-LLH_glcm_Idn and wavelet-LLH_glcm_Idmn, indicating that increase of tumor homogeneity may be associated with worse prognosis, consistent with findings in recent radiomics based lung cancer survival study (35). Moreover, the change of number/ratio of small zones shows negative correlation with the variation of increased risks, such as original_glszm_ZonePercentage, indicating that smaller size of tumor zone and more fine textures tend to show better therapeutic effects of SBRT. Such observations are also supported by visual inspection of tumor images, such as those shown in Figure 4 (b).

The findings of this analysis demonstrate the ability to achieve individual patient risk and outcome stratification that supports the use of radiomics to guide clinical decision-making. This is particularly important for ES-NSCLC due to the high rates of regional and distant failures, even among patients who achieved local control. As such, future investigation validating these findings may identify which ES-NSCLC patients are most likely to benefit from systemic therapy in conjunction with SBRT. This is clinically meaningful, as large reports have suggested that adding chemotherapy to SBRT may improve survival in higher risk ES-NSCLC patients (51). Additionally, with increasing recognition of a potential synergy between immunotherapy and radiotherapy, and particularly SBRT, strategies such as this analysis that identify higher risk patients may optimally identify ES-NSCLC patients that may benefit from adding immunotherapy to SBRT, which is the subject of the ongoing SWOG/NRG Oncology intergroup S1914 trial and RTOG Foundation PACIFIC-4 trial (52).

While this study was of a large, homogenous dataset assessing numerous tumor characteristics assessed using robust analyses methods, the present study has several limitations. First, the prediction model was validated on an independent dataset from the same institute. Validation studies based on large, external datasets are needed to evaluate the proposed method more rigorously and will be the subject of future analyses. Second, the training data only had pre-treatment CT scans and, therefore, we were not able to build delta-radiomics prediction models for a direct comparison. Third, our study had moderate sample size and included a small number of demographic and clinical measures, especially compared with several recent large scale studies which investigated several hundreds of patients and included a rich set of clinical measures (53,54). It is expected that an effective integration of radiomic features and rich clinical information will further improve the prediction performance. Fourth, all the tumors were manually contoured by experienced radiation oncologists. However, we did not evaluate inter-observer variability. A high inter-observer variability may degrade the reproducibility of the extracted radiomic features.

In conclusion, we presented a new and effective means to integrate pre- and post-treatment imaging data for predicting clinical outcomes of ES-NSCLC patients treated with SBRT. This method may help identify early stage NSCLC patients treated with SBRT who may benefit from adjuvant treatment.

Supplementary Material

Refer to Web version on PubMed Central for supplementary material.

Acknowledgments

Funding statement

Research reported in this study was supported by the National Cancer Institute of the National Institutes of Health under award number of CA223358. The content is solely the responsibility of the authors and does not necessarily represent the official views of the National Institutes of Health.

Conflicts of interest

Dr. Pryma reports grants and personal fees from Siemens AG, grants and personal fees from 511 Pharma, grants from Progenics Pharmaceuticals Inc, personal fees from Bayer, during the conduct of the study.

Dr. Aggarwal reports grants from AZ, Incyte, and Merck, and personal fees from AZ, BMS, Celgene, EliLilly, Merck, Roche.

Dr. Kao is a co-founder and has equity in Liquid Biotech USA, Inc., a University of Pennsylvania PCI-developed company through the UPStart program.

All other authors have nothing to disclose.

References

1. Howlader N, Noone A, Krapcho M, et al. Seer cancer statistics review, 1975–2016. National Cancer Institute 2019.
2. Ettinger DS, Akerley W, Borghaei H, et al. Non–small cell lung cancer. Journal of the National Comprehensive Cancer Network 2012;10:1236–1271. [PubMed: 23054877]
3. Siegel RL, Miller KD, Jemal A. Cancer statistics, 2020. CA Cancer J Clin 2020;70:7–30. [PubMed: 31912902]
4. Investigators IELCAP. Survival of patients with stage i lung cancer detected on ct screening. New England Journal of Medicine 2006;355:1763–1771.
5. Kovalchik SA, Tammemagi M, Berg CD, et al. Targeting of low-dose ct screening according to the risk of lung-cancer death. New England Journal of Medicine 2013;369:245–254.
6. Palma D, Visser O, Lagerwaard FJ, et al. Impact of introducing stereotactic lung radiotherapy for elderly patients with stage i non–small-cell lung cancer: A population-based time-trend analysis. Journal of clinical oncology 2010;28:5153–5159. [PubMed: 21041709]
7. Kapadia NS, Valle LF, George JA, et al. Patterns of treatment and outcomes for definitive therapy of early stage non-small cell lung cancer. The Annals of thoracic surgery 2017;104:1881–1888. [PubMed: 29106887]
8. Shah JL, Loo BW Jr. Stereotactic ablative radiotherapy for early-stage lung cancer. Seminars in radiation oncology 2017;27:218–228. [PubMed: 28577829]
9. Choi JI, Simone CB 2nd. Stereotactic body radiation therapy versus surgery for early stage non-small cell lung cancer: Clearing a path through an evolving treatment landscape. J Thorac Dis 2019;11:S1360–S1365. [PubMed: 31245133]
10. Videtic GMM, Donington J, Giuliani M, et al. Stereotactic body radiation therapy for early-stage non-small cell lung cancer: Executive summary of an astro evidence-based guideline. Pract Radiat Oncol 2017;7:295–301. [PubMed: 28596092]
11. Chang JY, Senan S, Paul MA, et al. Stereotactic ablative radiotherapy versus lobectomy for operable stage i non-small-cell lung cancer: A pooled analysis of two randomised trials. Lancet Oncol 2015;16:630–7. [PubMed: 25981812]
12. Timmerman RD, Paulus R, Pass HI, et al. Stereotactic body radiation therapy for operable early-stage lung cancer: Findings from the nrg oncology rtog 0618 trial. JAMA Oncol 2018;4:1263–1266. [PubMed: 29852037]
13. Palma DA, Nguyen TK, Louie AV, et al. Measuring the integration of stereotactic ablative radiotherapy plus surgery for early-stage non-small cell lung cancer: A phase 2 clinical trial. JAMA Oncol 2019;5:681–688. [PubMed: 30789648]
14. Vachani A, Sequist LV, Spira A. Ajrccm: 100-year anniversary. The shifting landscape for lung cancer: Past, present, and future. Am J Respir Crit Care Med 2017;195:1150–1160. [PubMed: 28459327]
15. Lim C, Sekhon HS, Cutz JC, et al. Improving molecular testing and personalized medicine in non-small-cell lung cancer in ontario. Curr Oncol 2017;24:103–110. [PubMed: 28490924]
16. Kong FS, Hirsch FR, Machtay M. Potential future consideration for imaging and blood-based biomarkers for precision medicine in lung cancer. Transl Lung Cancer Res 2017;6:713–715. [PubMed: 29218273]
17. Lambin P, Rios-Velazquez E, Leijenaar R, et al. Radiomics: Extracting more information from medical images using advanced feature analysis. European journal of cancer 2012;48:441–6. [PubMed: 22257792]

18. Kumar V, Gu Y, Basu S, et al. Radiomics: The process and the challenges. Magnetic resonance imaging 2012;30:1234–48. [PubMed: 22898692]
19. Lambin P, Leijenaar RTH, Deist TM, et al. Radiomics: The bridge between medical imaging and personalized medicine. Nature Reviews Clinical Oncology 2017;14:749.
20. Gillies RJ, Kinahan PE, Hricak H. Radiomics: Images are more than pictures, they are data. Radiology 2016;278:563–577. [PubMed: 26579733]
21. Starkov P, Aguilera TA, Golden DI, et al. The use of texture-based radiomics ct analysis to predict outcomes in early-stage non-small cell lung cancer treated with stereotactic ablative radiotherapy. The British Journal of Radiology 2019;92:20180228. [PubMed: 30457885]
22. Scrivener M, de Jong EE, van Timmeren JE, et al. Radiomics applied to lung cancer: A review. Translational Cancer Research 2016;5:398–409.
23. Chen B, Zhang R, Gan Y, et al. Development and clinical application of radiomics in lung cancer. Radiation oncology 2017;12:154. [PubMed: 28915902]
24. Constanzo J, Wei L, Tseng H-H, et al. Radiomics in precision medicine for lung cancer. Translational Lung Cancer Research 2017;6:635–647. [PubMed: 29218267]
25. Coroller TP, Grossmann P, Hou Y, et al. Ct-based radiomic signature predicts distant metastasis in lung adenocarcinoma. Radiotherapy and Oncology 2015;114:345–350. [PubMed: 25746350]
26. Huang Y, Liu Z, He L, et al. Radiomics signature: A potential biomarker for the prediction of disease-free survival in early-stage (i or ii) non—small cell lung cancer. Radiology 2016;281:947–957. [PubMed: 27347764]
27. Lee G, Lee HY, Park H, et al. Radiomics and its emerging role in lung cancer research, imaging biomarkers and clinical management: State of the art. European journal of radiology 2017;86:297–307. [PubMed: 27638103]
28. Mattonen SA, Palma DA, Johnson C, et al. Detection of local cancer recurrence after stereotactic ablative radiation therapy for lung cancer: Physician performance versus radiomic assessment. International Journal of Radiation Oncology* Biology* Physics 2016;94:1121–1128.
29. Sampath S, Rahmanuddin S, Sahoo P, et al. Change in apparent diffusion coefficient is associated with local failure after stereotactic body radiation therapy for non-small cell lung cancer: A prospective clinical trial. International Journal of Radiation Oncology* Biology* Physics 2019;105:659–663.
30. Li H, Galperin-Aizenberg M, Pryma D, et al. Unsupervised machine learning of radiomic features for predicting treatment response and overall survival of early stage non-small cell lung cancer patients treated with stereotactic body radiation therapy. Radiotherapy and Oncology 2018;129:218–226. [PubMed: 30473058]
31. Hawkins SH, Korecki JN, Balagurunathan Y, et al. Predicting outcomes of nonsmall cell lung cancer using ct image features. IEEE Access 2014;2:1418–1426.
32. Li Q, Kim J, Balagurunathan Y, et al. Imaging features from pretreatment ct scans are associated with clinical outcomes in nonsmall-cell lung cancer patients treated with stereotactic body radiotherapy. Medical physics 2017;44:4341–4349. [PubMed: 28464316]
33. Vaidya M, Creach KM, Frye J, et al. Combined pet/ct image characteristics for radiotherapy tumor response in lung cancer. Radiotherapy and oncology : journal of the European Society for Therapeutic Radiology and Oncology 2012;102:239–45. [PubMed: 22098794]
34. Desseroit MC, Visvikis D, Tixier F, et al. Development of a nomogram combining clinical staging with (18)f-fdg pet/ct image features in non-small-cell lung cancer stage i-iii. European journal of nuclear medicine and molecular imaging 2016;43:1477–85. [PubMed: 26896298]
35. Yu W, Tang C, Hobbs BP, et al. Development and validation of a predictive radiomics model for clinical outcomes in stage i non-small cell lung cancer. International Journal of Radiation Oncology* Biology* Physics 2018;102:1090–1097.
36. Plautz TE, Zheng C, Noid G, et al. Time stability of delta-radiomics features and the impact on patient analysis in longitudinal ct images. Medical physics 2019;46:1663–1676. [PubMed: 30695103]
37. Fave X, Zhang L, Yang J, et al. Delta-radiomics features for the prediction of patient outcomes in non–small cell lung cancer. Scientific Reports 2017;7:588. [PubMed: 28373718]

38. Cunliffe A, Armato SG 3rd, Castillo R, et al. Lung texture in serial thoracic computed tomography scans: Correlation of radiomics-based features with radiation therapy dose and radiation pneumonitis development. Int J Radiat Oncol Biol Phys 2015;91:1048–56. [PubMed: 25670540]
39. Bak SH, Park H, Sohn I, et al. Prognostic impact of longitudinal monitoring of radiomic features in patients with advanced non-small cell lung cancer. Sci Rep 2019;9:8730. [PubMed: 31217441]
40. Aerts HJ, Velazquez ER, Leijenaar RT, et al. Decoding tumour phenotype by noninvasive imaging using a quantitative radiomics approach. Nature communications 2014;5:1–9.
41. De Petris L, Lax I, Sirzén F, et al. Role of gross tumor volume on outcome and of dose parameters on toxicity of patients undergoing chemoradiotherapy for locally advanced non-small cell lung cancer. Medical Oncology 2005;22:375–381. [PubMed: 16260855]
42. Wang W, Xu Y, Schipper M, et al. Effect of normal lung definition on lung dosimetry and lung toxicity prediction in radiation therapy treatment planning. International Journal of Radiation Oncology* Biology* Physics 2013;86:956–963.
43. Van Griethuysen JJ, Fedorov A, Parmar C, et al. Computational radiomics system to decode the radiographic phenotype. Cancer research 2017;77:e104–e107. [PubMed: 29092951]
44. Hosny A, Parmar C, Coroller TP, et al. Deep learning for lung cancer prognostication: A retrospective multi-cohort radiomics study. PLoS medicine 2018;15:e1002711. [PubMed: 30500819]
45. Ishwaran H, Kogalur UB, Blackstone EH, et al. Random survival forests. The annals of applied statistics 2008;2:841–860.
46. Harrell FE Jr, Lee KL, Mark DB. Multivariable prognostic models: Issues in developing models, evaluating assumptions and adequacy, and measuring and reducing errors. Statistics in medicine 1996;15:361–387. [PubMed: 8668867]
47. Pedregosa F, Varoquaux G, Gramfort A, et al. Scikit-learn: Machine learning in python. the Journal of machine Learning research 2011;12:2825–2830.
48. Parmar C, Grossmann P, Bussink J, et al. Machine learning methods for quantitative radiomic biomarkers. Scientific reports 2015;5:13087. [PubMed: 26278466]
49. Ishwaran H Variable importance in binary regression trees and forests. Electronic Journal of Statistics 2007;1:519–537.
50. Breiman L Random forests. Machine learning 2001;45:5–32.
51. Verma V, McMillan MT, Grover S, et al. Stereotactic body radiation therapy and the influence of chemotherapy on overall survival for large (≥ 5 centimeter) non-small cell lung cancer. International Journal of Radiation Oncology* Biology* Physics 2017;97:146–154.
52. Fitzgerald K, Simone CB. Combining immunotherapy with radiation therapy in non–small cell lung cancer. Thoracic Surgery Clinics 2020;30:221–239. [PubMed: 32327181]
53. Kang J, Ning MS, Feng H, et al. Predicting 5-year progression and survival outcomes for early stage non-small cell lung cancer treated with stereotactic ablative radiation therapy: Development and validation of robust prognostic nomograms. International Journal of Radiation Oncology, Biology, Physics 2020;106:90–99.
54. Louie AV, Haasbeek CJA, Mokhles S, et al. Predicting overall survival after stereotactic ablative radiation therapy in early-stage lung cancer: Development and external validation of the amsterdam prognostic model. International Journal of Radiation Oncology, Biology, Physics 2015;93:82–90.

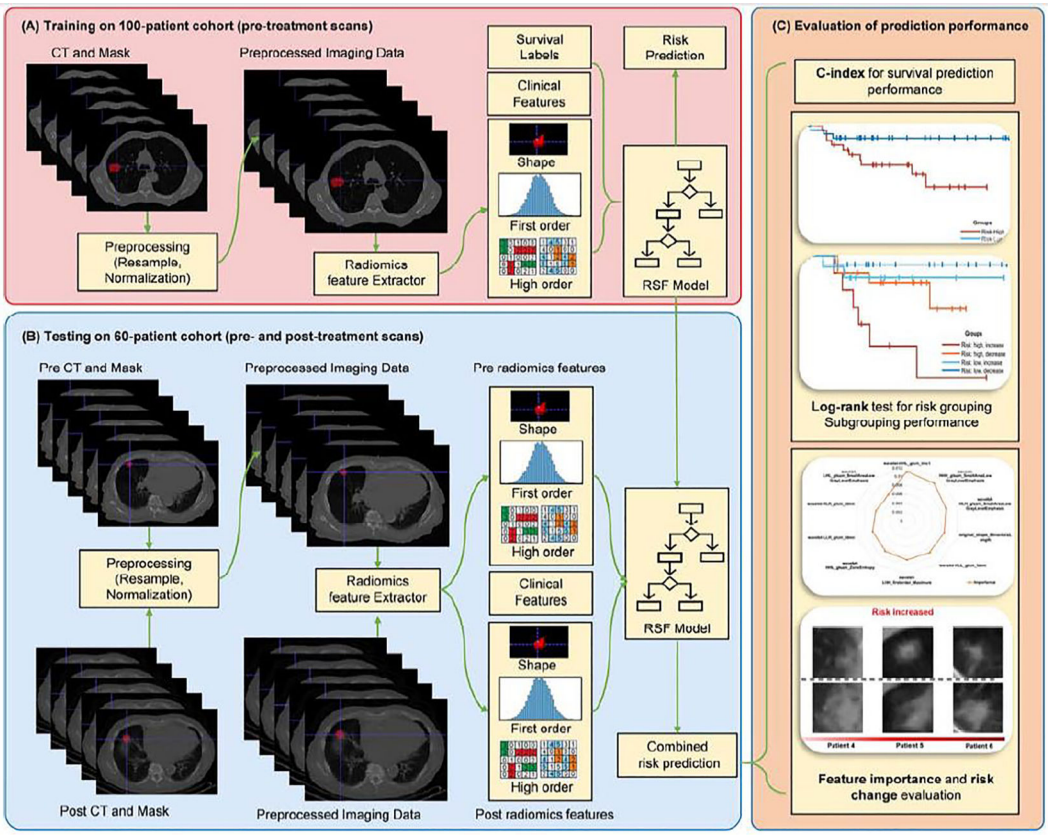

Figure 1.

Flowchart of the prediction modeling method. (A) Construction of a prediction model based on the 100-patient cohort; (B) Application of the prediction model to the 60-patient cohort; (C) Stratification of patients based on predicted risk scores.

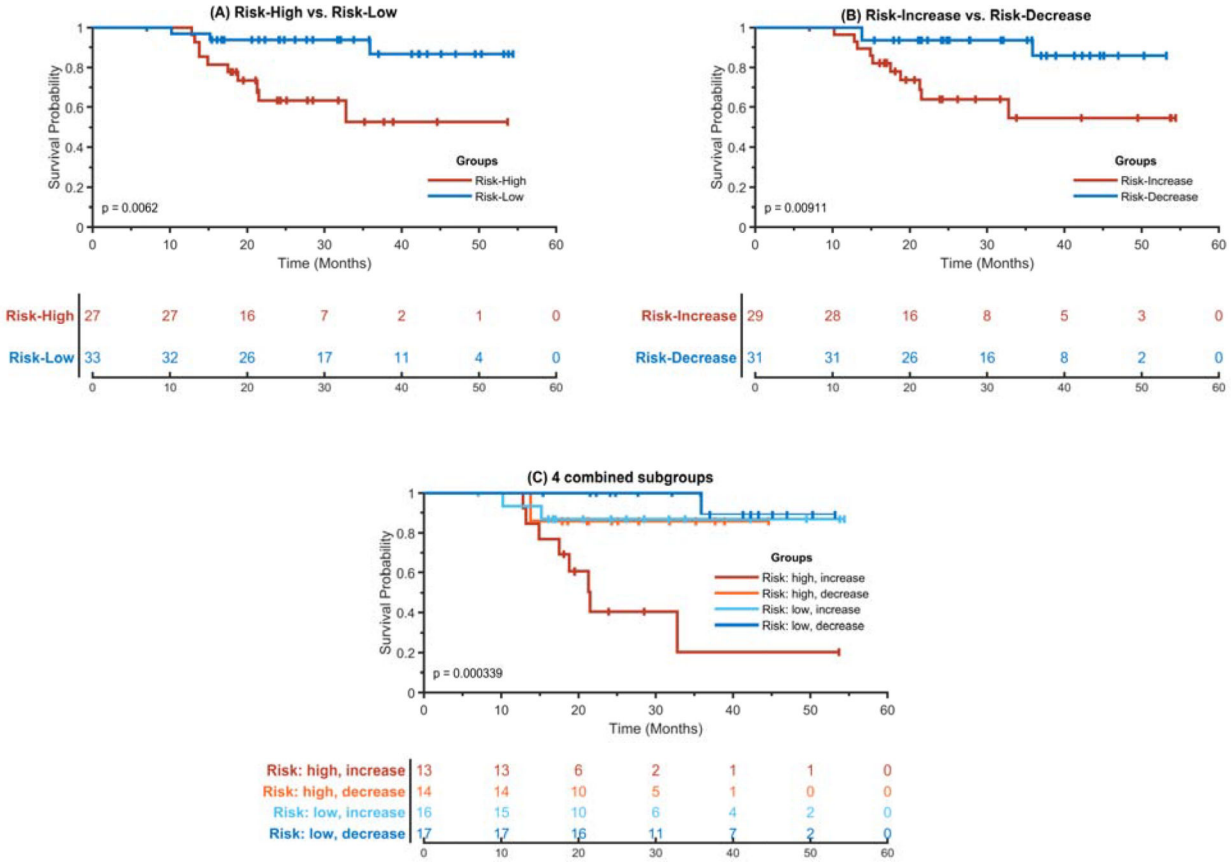

Figure 2.

Kaplan-Meier plots of stratified risk subgroups. (A) Risk-High vs. Risk-Low. (B) Risk-Increase vs. Risk-Decreased. (C) 4 combined subgroups. In all the plots, the x-axis represents survival time in months and the y-axis represents the survival probability. Lines in different colors represent different risk groups and subgroups, and "+" in these lines are censored instances. The Risk-High and Risk-Low subgroups were identified based on a cut-off point of risk scores of individual patients, and the Risk-increase and Risk-Decrease subgroups were defined based on changes of risk scores of pre- and posttreatment CT scans of individual patients.

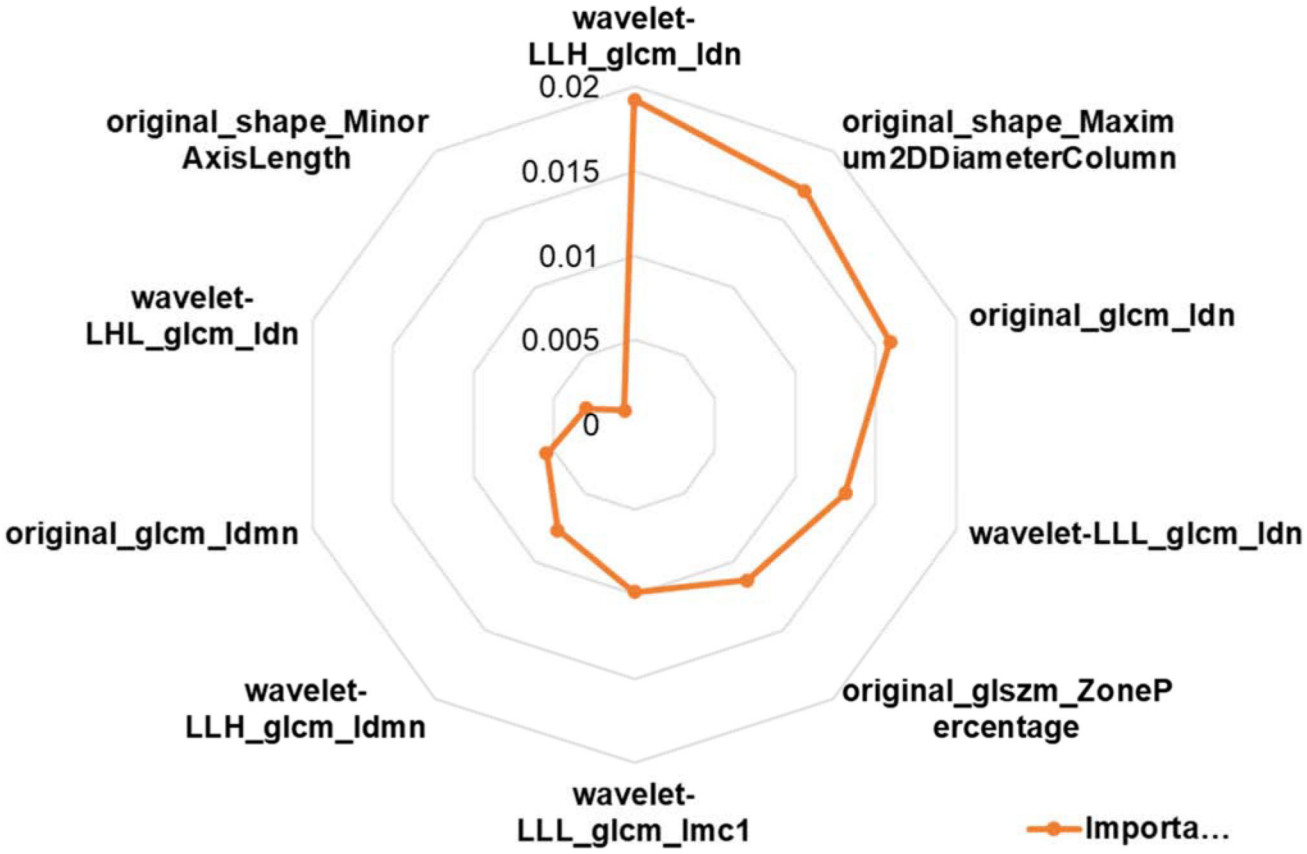

Figure 3.
Radar plot of top 10 most important radiomics features for survival prediction.

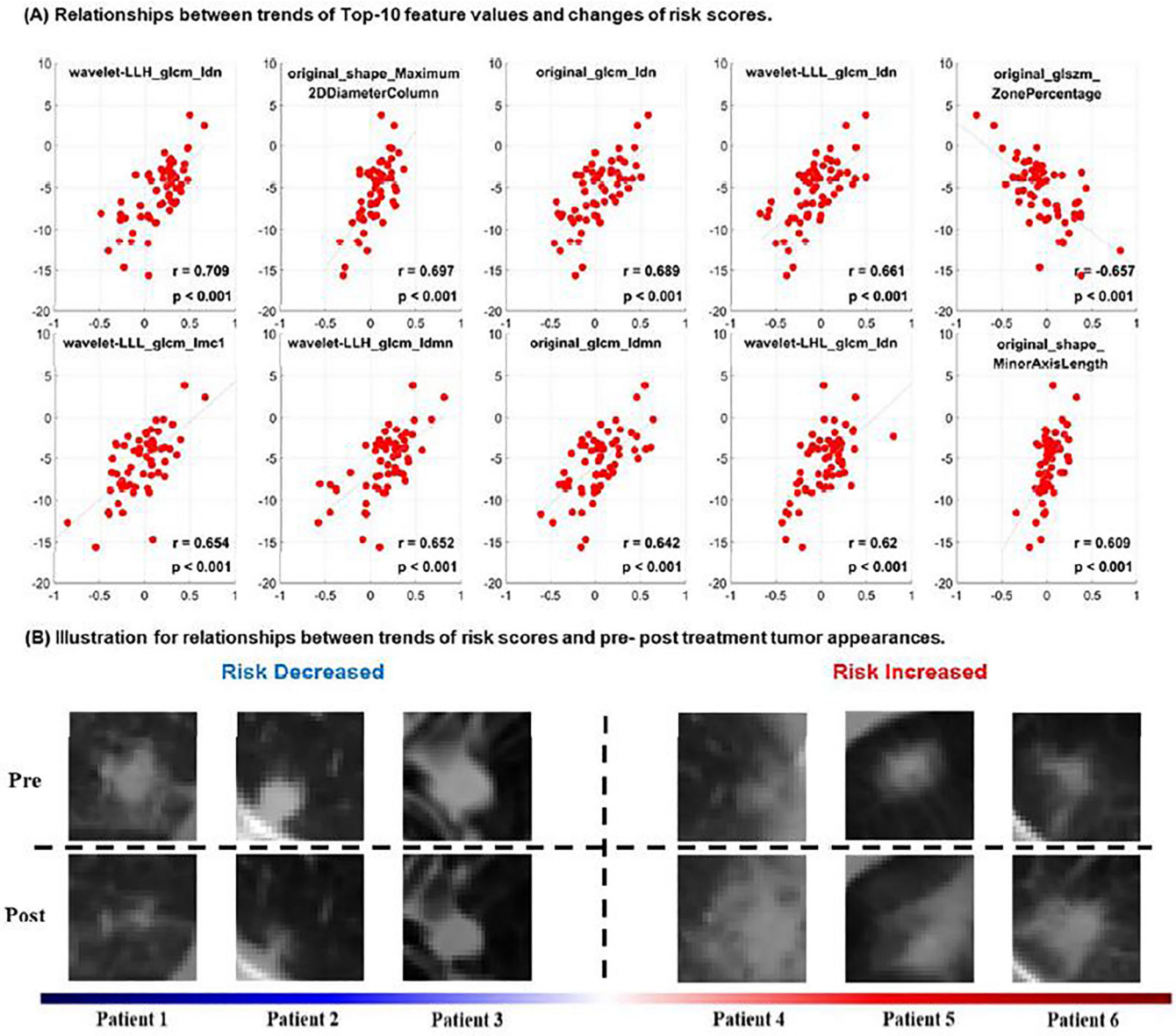

Figure 4.

Quantitative correlation analysis of changes in radiomic features with change in risk scores and visual inspection of changes in tumor images before and after SBRT. (A) Relationships between trends of Top-10 feature values and changes of risk scores estimated from pre- and post-treatment CT scans. (B) pre-treatment (top row) and post-treatment (bottom row) tumor CT scans of representative patients with increased or decreased risk scores after SBRT treatment.

Table 1.

Demographic data and clinical characteristics of ES-NSCLC patients.

Characters	100-patient cohort	60-patient cohort	p value
Age (Years)	70.6±11.8	71.7±9.1	0.529
Sex (M/F)	48%/52%	38%/62%	0.236
Current or former smoker	96%	97%	0.831
BMI ± Standard Deviation	27.5±6.4	26.5±5.8	0.325
Deceased	39%	22%	<0.001
Local Failure	7%	18%	0.304
Nodal Failure	17%	18%	0.323
Distant Failure	9%	17%	0.946
Mean tumor size ± Standard Deviation (cm^3)	1.99±0.87	1.77±0.80	0.105
Mean, median follow-up time (Month)	19.0, 16.4	28.6, 25.0	<0.001
Range of follow-up time (Month)	[2.1, 47.8]	[7, 54.4]	
Median of prescription dose (Gy)	50	50	
BED10 (Gy)	100/112.5 (5/4 fractions)	100/112.5 (5/4 fractions)	

Table 2.

Overall survival differences between pairs of 4 subgroups of ES-NSCLC patients who were significantly different in overall survival (χ^2 = 18.549.623, p=3.4e-04, log-rank test).

Pairs of subgroups	χ^2	p value
Risk: high+ increased vs. Risk: high + decreased	5.62	0.018
Risk: high+ increased vs. Risk: low + increased	5.84	0.016
Risk: high+ increased vs. Risk: low+ decreased	15.45	8.5e-5
Risk: high + decreased vs. Risk: low + increased	0.03	0.955
Risk: high + decreased vs. Risk: low + decreased	1.08	0.300
Risk: low + increased vs. Risk: low + decreased	0.84	0.360